International Conference
ENGINEERING MECHANICS 2010
Svratka, Czech Republic, May 10 – 13, 2010

NONLINEAR ANALYSIS OF THE INTERACTION OF THE STEEL LINER AND REINFORCED CONCRETE WALL OF THE BUBBLER TOWER DUE TO EXTREME PRESSURE AND TEMPERATURE

J. Králik*, D. Hukel*

Summary: *This paper describes the nonlinear analysis of the reinforced concrete wall of the bubbler tower (BT) due to extreme pressure and temperature loading. The behaviour of the pressure and temperature in hermetic zone was simulated by program MELCOR. The interaction of the steel liner and reinforced concrete wall during the loss of coolant accident is considered. The new layered shell element of the reinforced concrete wall was developed. On the base of the experimental results and the nonlinear analysis of the structure were considered the safety and reliability of the structure. The numerical simulations were realized in the system ANSYS and CRACK.*

1. Introduction

The International Atomic Energy Agency set up a program (IAEA, 1995) to give guidance to its member states on the many aspects of the safety of nuclear power reactors. The resistance of the buil-ding structure must be checked for extreme steam pressure in the case of small or medium-sized accidents, such as a Loss of Coolant Accident (LOCA) or a High Energy Line Break (HELB) or a Steam Line Break Accident (SBLA) on the other primary loop piping system. Compliance with the IAEA (1995) and Eurocode (1990, 1992) will be considered in three load combinations: Normal Conditions (NOC), Design Basic Accident (DBA) and Beyond Design Basic Accident (BDBA).

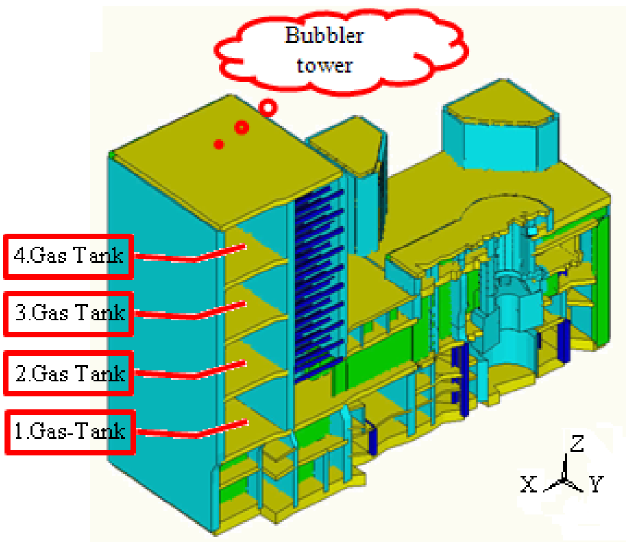

Figure 1 Calculation FEM model of NPP V2

* Assoc. Prof. Ing. Juraj Králik, CSc., Ing. Dušan Hukel : Department of Structural Mechanics, Faculty of Civil Engineering, Slovak Univerzity of Technology in Bratislava; Radlinského 11; 813 68 Bratislava; tel.: +421 (2) 50 274 690, fax: +421 (2) 52 494 332; e-mail: juraj.kralik@stuba.sk

On the base of the IAEA requirements the experimental test of the airtightness of hermetic zone must be realized each 10 years of NPP performance. The stiffness of structure is tested during this experiment too.

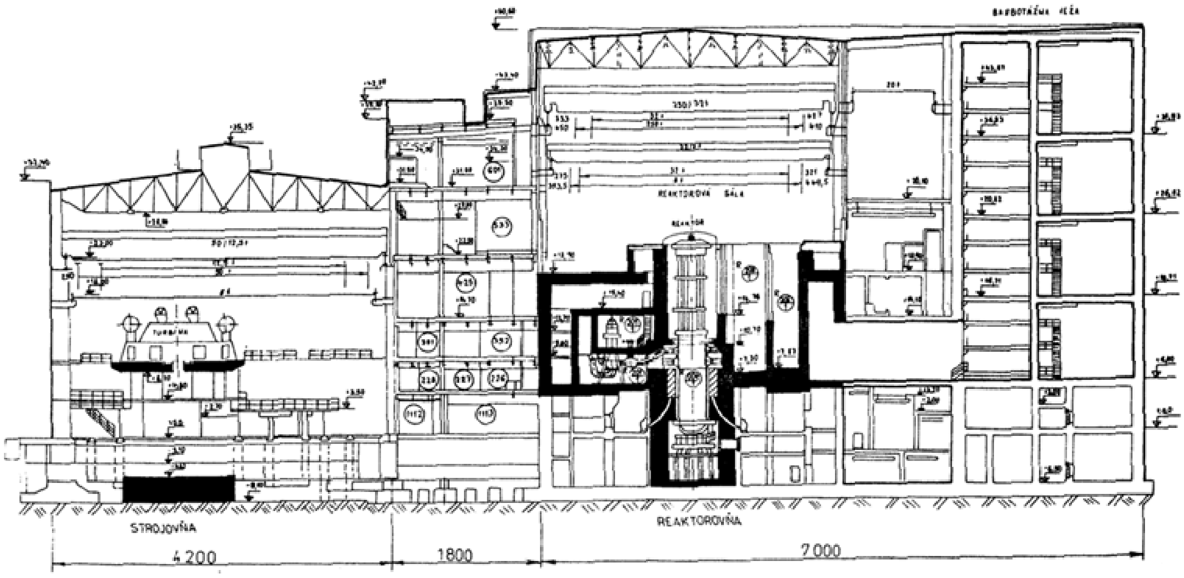

Figure 2 Cross section of the nuclear power plant buildings type V2

The experimental results were compared with the results of numerical analysis of the structures on the FEM calculation model. For a complex analysis of the concrete structure for different kind of loads, ANSYS software and the program CRACK (Králik, 2001, 2002, 2002a, 2009) were provided to solve this task. The building of the power block was idealized with a discrete model consisting of 28 068 elements with 104 287 DOF (see Fig.1).

2. Experimental test of the airtightness and the stiffness

The airtightness of the hermetic zone and the stiffness resistance of the structures were tested by compression of the interior space of NPP. The pressure increase from the 0kPa to 100kPa and since the pressure decrease to 0kPa with the same tempo. The results of the measurements were recorded at pressure 0, 25, 50, 75 and 100kPa.

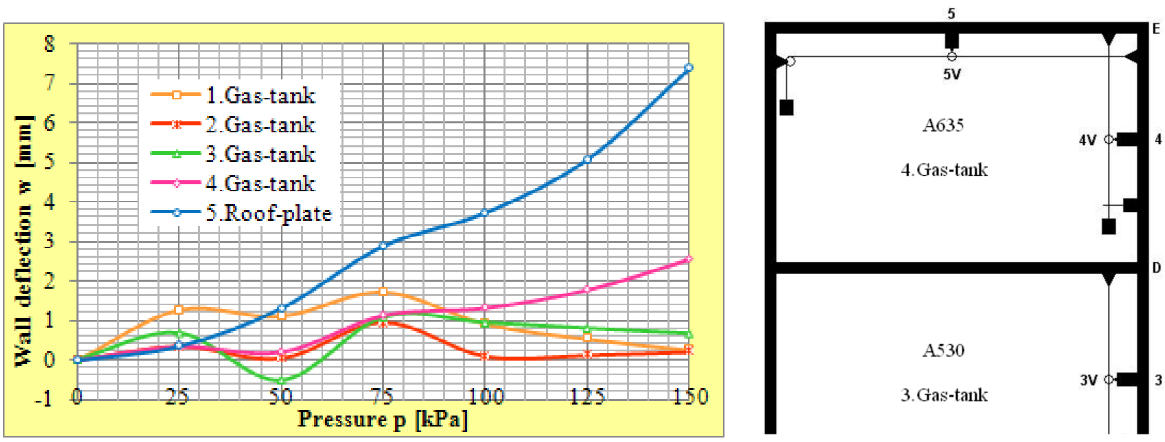

Figure 3 Extrapolated behavior of relative displacements of the wall at modulus „*E*“ and roof plate at point 1 to 5

The inspection of the critical places was realized by the experts (STU Bratislava, VUEZ

Levice, VUJE Trnava, SE Bratislava) after each changing step (Kralik, 2009). The optical and mechanical methods were used to check the deformation of structures in the critical places during the pressure change into hermetic zone. The critical places of the structures were determined by the numerical analysis. The mechanical indicators were installed in the wall centre of the gas-tank and the roof-plate of the bubbler tower (see Fig.3b). The mechanical indicators were fixed with cable system in interior of BT. The optical measurements were realized from the exterior by LIPG Bratislava. The results of the measurements were recorded at pressure 0, 25, 50, 75 and 100kPa. The optical and the mechanical methods were used to check the deformation of the structures in the critical places during the pressure change inside the hermetic zone.

3. Scenario for LOCA loads

The safety and reliability of the NPP structures of the hermetic zone must be tested on the resistance to the LOCA accident (NUREG-1150, 1990). The DBA a BDBA loads were defined from the scenarios of the guillotine cutting of the ∅13mm, ∅32mm, ∅71mm and 2x∅500mm cold leg in the Box SG. The peaks pressure and temperature were considered on the base of the scenarios in program MELCOR by VUJE Trnava (Juriš, Jančovič, 2006).

The temperature in the containment increased during the LOCA accident. The peaks of the temperature are equal to 160°C in the Box SG (Steam generator) by the results of thermodynamic analysis. The effect of these temperature peaks is minimal during the accident and the acting of the overpressure loads. In the case of the harmonic amplitude of temperature the phase angle for concrete walls is superior to 24 hours. The strength of the concrete after LOCA accident increases about to 10% in consequence of the temperature loads during the accident (Janotka, Nűrnbergerová, 1999). The peak of the pressure in the Box SG is equal to 200kPa (absolute value).

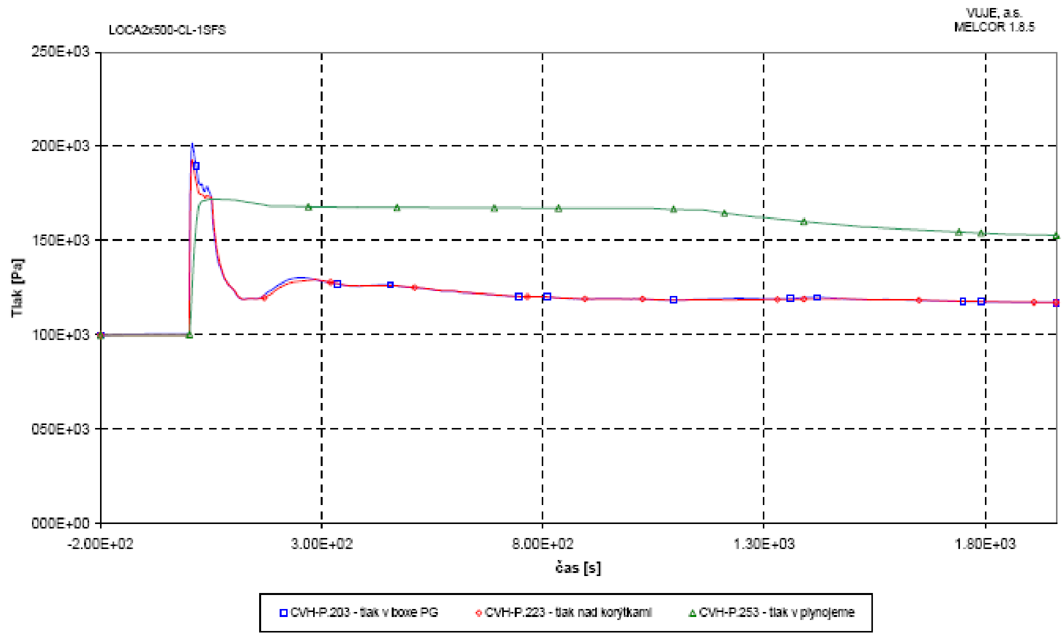

Figure 4 Overpression in the Box SG for guillotine cutting of pipe 2x∅500mm

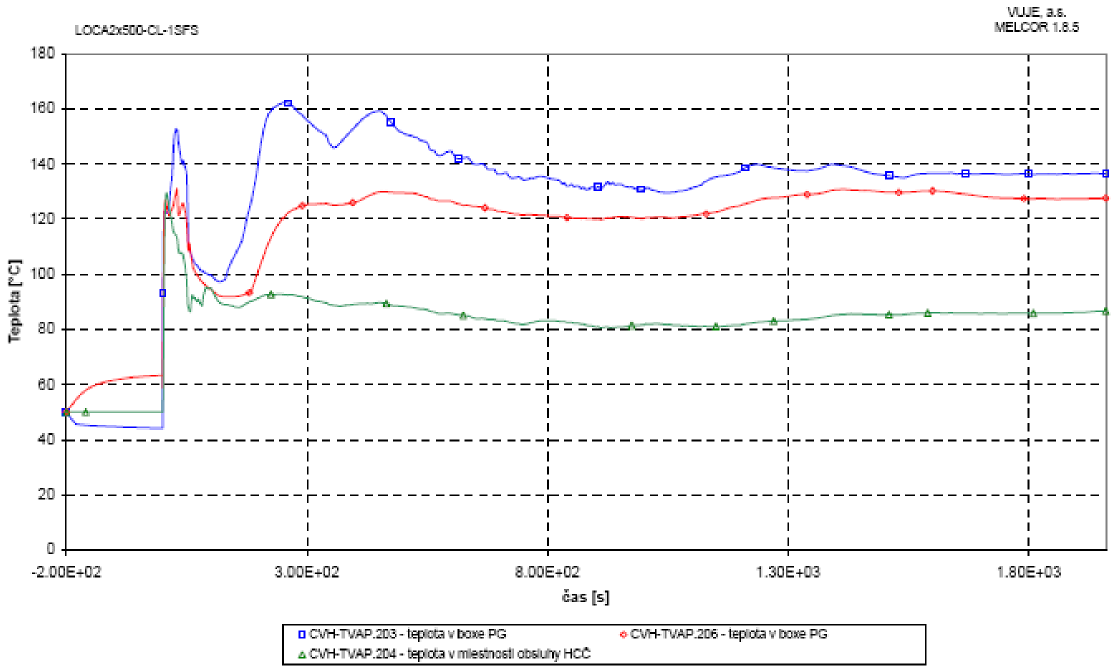

Figure 5 Temperature in the Box SG for guillotine cutting of pipe 2x∅500mm

4. Numerical analysis of bubbler tower resistance

The BDBA load case (IAEA, 1995) was defined for the pressure 0,150MPa following

$$E = D + L + P_a + 0{,}7.T_o + R_a, \qquad (1)$$

were D - dead loads, L - live loads, T_o - performance temperature, R_a - reaction of the equipments, P_a - local effects of the LOCA.

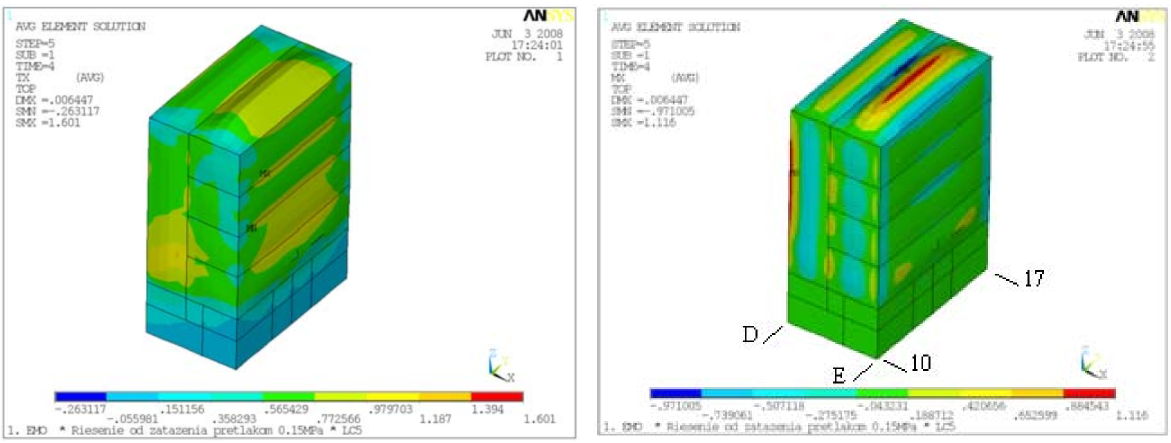

Figure 6 Normal forces t_x and bending moments m_x under pressure 0,150MPa

The behaviour of the intensity of normal forces t_x and bending moments m_x under pressure 150kPa is presented in Fig.3. The most exposed walls on the tension are the walls in the modulus "10" and "17" and wall bottom in the modulus "*E*". The roof plate of the gas-tank is exposed on the tension too (Fig.3a). The most exposed walls on the bending are the walls in the modulus “10” and “17” in the corner with wall in module “*D*”. and wall bottom in the modulus “*E*”. The roof plate of the gas-tank is exposed on the bending too (Fig.3b).

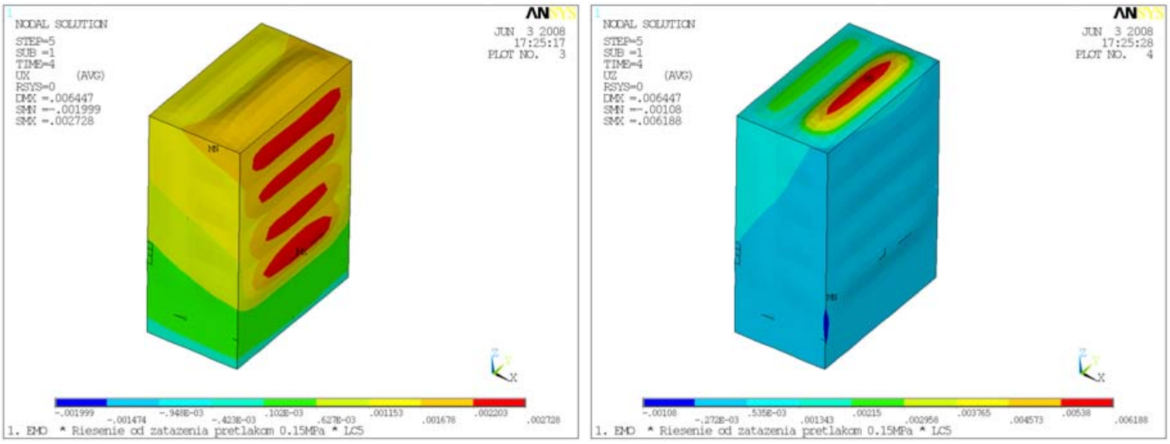

Figure 7 Deformation shape of the BT wall in direction X and Z under pressure 0,150MPa

The deformation shape of the BT structures (Fig.7) under pressure 0,150MPa show us that the peak values of the horizontal displacements are in the walls at modulus *E* and the maximum vertical displacements are in the roof plate.

Table 1 The internal forces of the BT critical structures on 3D model (Fig.6)

	Roof plate at +50,6m			Wall at modulus *E* (4.gas tank)		
Load case	*N* [MN/m]	*M*[MN/m]	Využitie %	*N* [MN/m]	*M* [MN/m]	Využitie %
Overpressure 150kPa	2,002	0,390	47,35	0,730 0,577	0,031 0,168	33,71 16,22
BDBA(load.combin.)	0,655	-0,103	14,86	1,139 0,670	2,139 2,187	84,33 76,79

Notes – N is the normal forces at plane ZX, M is the bending moment at plane ZX.

Table 2 The displacements BT critical structures on 3D model (Fig.7)

	Roof plate at +50,6m			Wall at modulus *E* (4. gas tank)		
Load case	w_{tot} [mm]	w_{rel} [mm]	ratio [%]	w_{tot} [mm]	w_{rel} [mm]	ratio [%]
Overpressure 150kPa	6,175	5,279	85	2,446	0,387	16
BDBA(load.combin.)	4,196	4,751	113	8,788	1,848	21

Notes – w_{tot} *is the total deflection,* w_{rel} *is the relative deflection in the wall centre (between two floors).*

The results in the Table 1 present that the maximum tension effect is in the roof plate at level +50,6m due to overpressure 150kPa. The effect of the overpressure is reduced due to the performance temperature in the roof plate. The load combination BDBA has the unfavourable impact to the BT wall at modulus *E*.

The comparison of the absolute and relative deflections of the 4th gas tank wall centre due to overpressure 150kPa and the load combination BDBA in 3D FEM model is presented in table 2. The influence of the temperature is against to the overpressure impact in the case of the roof plate (Table 2). The load combination BDBA has an adverse effect as other to the wall deflection.

4. Nonlinear FEM model of the reinforced concrete layered shell

During the increasing of the extreme overpressure inside the hermetic zone the process of the cracking and crushing are expanded in the reinforced concrete walls (FISA99 - 1995, Králik, Cesnak - 2001). These effects must be considered using nonlinear FEM model of the reinforced concrete structure (Materna et al, 2000).

The presented constitutive model is a further extension of the smeared crack model (Oňate et al, 1988), which was developed in (Králik, Cesnak, 2001). Following the experimental results of Červenka (1985), Kupfer (1969), Jerga and Križma (2006), and others (FISA99, 1999) a new concrete cracking layered finite shell element (Králik, Cesnak, 2001) was developed and incorporated into the ANSYS system (Králik, 2009). The layered approximation, the smeared steel reinforcement and smeared crack model of the shell element are proposed.

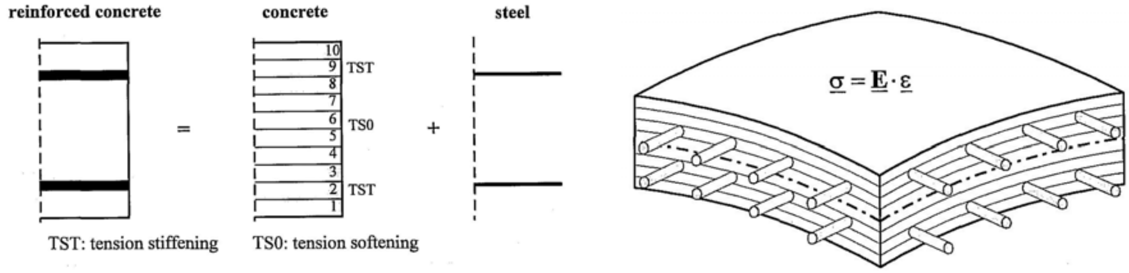

Figure 8 Layered approximation of the reinforced concrete shell

The processes of the concrete cracking and crushing are developed during the increasing of the load. The concrete compressive stress f_c, the concrete tensile stress f_t and the shear modulus G are reduced after the crushing or cracking of the concrete (Červenka, 1985).

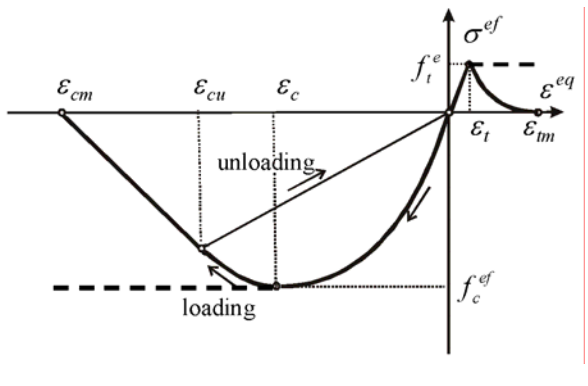

Figure 9 The concrete stress-strain diagram

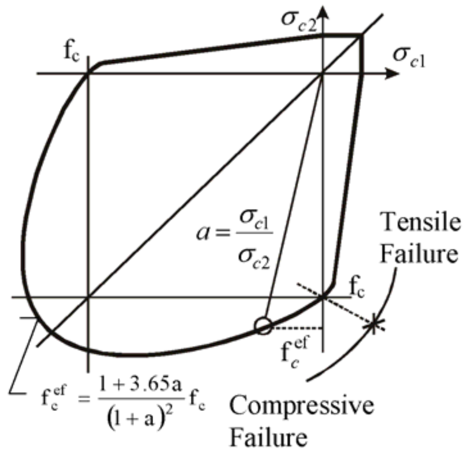

Figure 10 Kupfer's plasticity function

In the case of the plane state the strength function in tension f_t and in compression f_c were considered equivalent values f_t^{eq} and f_c^{eq}. In the plane of principal stresses (σ_{c1}, σ_{c2}) the relation between the one and bidimensional stresses state due to the plasticity function by Kupfer (1969) can be defined as follows (see Figure 5):

➲ Compression-compression

$$f_c^{ef} = \frac{1+3.65.a}{(1+a)^2}.f_c, \qquad a = \frac{\sigma_{c1}}{\sigma_{c2}} \tag{2}$$

➲ Tension-compression

$$f_c^{ef} = f_c . r_{ec},\ r_{ec} = \left(1 + 5.3278 \frac{\sigma_{c1}}{f_c}\right),\ r_{ec} \geq 0.9 \tag{3}$$

➲ Tension-tension

$$f_t^{ef} = f_t . r_{et}, \quad r_{et} = \frac{A + (A-1).B}{A.B}, \quad B = K.x + A, \quad x = \sigma_{c2} / f_c, \tag{4}$$

$$r_{et} = 1. \Leftrightarrow x = 0, \quad r_{et} = 0.2 \Leftrightarrow x = 1.$$

The shear concrete modulus G was defined for cracking concrete by Kolmar (1986) in the form

$$G = r_g . G_o,\ r_g = \frac{1}{c_2} \ln\left(\frac{\varepsilon_u}{c_1}\right), \quad c_1 = 7 + 333(p - 0.005), \quad c_2 = 10 - 167(p - 0.005), \tag{5}$$

where G_o is the initial shear modulus of concrete, ε_u is the strain in the normal direction to crack, c_1 and c_2 are the constants dependent on the ratio of reinforcing, p is the ratio of reinforcing transformed to the plane of the crack ($0 < p < 0.02$).

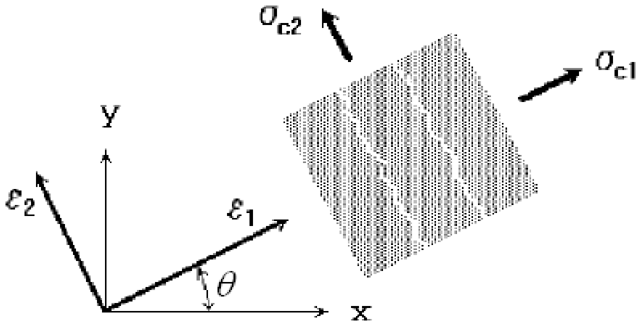

Figure 11 Rotated crack model of concrete

It is proposed that the crack in the one layer of shell element is oriented perpendicular to the orientation of principal stresses. The membrane stress and strain vector depends on the direction of the principal stress and strain in one layer

$$\{\varepsilon_{cr}\} = [T_\varepsilon]\{\varepsilon\}, \qquad \{\sigma_{cr}\} = [T_\sigma]\{\sigma\}, \tag{6}$$

where $[T_\varepsilon]$, $[T_\sigma]$ are transformation matrices for the principal strain and stress in the direction θ in the layer.

$$[T_\varepsilon] = \begin{bmatrix} \cos^2\theta & \sin^2\theta & \sin\theta\cos\theta & 0 & 0 \\ \sin^2\theta & \cos^2\theta & -\sin\theta\cos\theta & 0 & 0 \\ -2\sin\theta\cos\theta & 2\sin\theta\cos\theta & \cos 2\theta & 0 & 0 \\ 0 & 0 & 0 & \cos\theta & \sin\theta \\ 0 & 0 & 0 & -\sin\theta & \cos\theta \end{bmatrix} \tag{7}$$

$$[T_\sigma]=\begin{bmatrix} \cos^2\theta & \sin^2\theta & 2\sin\theta\cos\theta & 0 & 0 \\ \sin^2\theta & \cos^2\theta & -2\sin\theta\cos\theta & 0 & 0 \\ -\sin\theta\cos\theta & \sin\theta\cos\theta & \cos 2\theta & 0 & 0 \\ 0 & 0 & 0 & \cos\theta & \sin\theta \\ 0 & 0 & 0 & -\sin\theta & \cos\theta \end{bmatrix}$$

The strain-stress relationship in the Cartesian coordinates can be defined in dependency on the direction of the crack (in the direction of principal stress, versus strain)

$$[\sigma_{cr}]=[D_{cr}]\{\varepsilon_{cr}\} \quad \text{and therefore} \quad [\sigma]=[T_\sigma]^{\mathrm{T}}[D_{cr}][T_\varepsilon]\{\varepsilon\} \tag{8}$$

For the membrane and bending deformation of the reinforced concrete shell structure the layered shell element, on which a plane state of stress is proposed on every single layer, was used.

The stiffness matrix of the reinforced concrete for the l^{th}-layer can be written in the following form

$$\left[D_{cr}^{l}\right]=\left[T_{c.\sigma}^{l}\right]^{\mathrm{T}}\left[D_{c.cr}^{l}\right]\left[T_{c.\varepsilon}^{l}\right]+\sum_{s=1}^{Nrein}\left[T_{s}^{l}\right]^{\mathrm{T}}\left[D_{s}^{l}\right]\left[T_{s}^{l}\right] \tag{9}$$

where $[T_{c.\sigma}]$, $[T_{c.\varepsilon}]$, $[T_s]$ are the transformation matrices for the concrete and the reinforcement separately, *Nrein* is the number of the reinforcements in the l^{th}-layer.

After cracking the elasticity modulus and Poisson's ratio are reduced to zero in the direction perpendicular to the cracked plane, and a reduced shear modulus is employed. Considering 1 and 2 two principal directions in the plane of the structure, the stress-strain relationship for the concrete l^{th}-layer cracked in the 1-direction, is

$$\begin{Bmatrix} \sigma_1 \\ \sigma_2 \\ \tau_{12} \\ \tau_{13} \\ \tau_{23} \end{Bmatrix}_l = \begin{bmatrix} 0 & 0 & 0 & 0 & 0 \\ 0 & E & 0 & 0 & 0 \\ 0 & 0 & G_{12}^{cr} & 0 & 0 \\ 0 & 0 & 0 & G_{13}^{cr} & 0 \\ 0 & 0 & 0 & 0 & G_{23}^{cr} \end{bmatrix}_l \begin{Bmatrix} \varepsilon_1 \\ \varepsilon_2 \\ \gamma_{12} \\ \gamma_{13} \\ \gamma_{23} \end{Bmatrix}_l \tag{10}$$

where the shear moduli are reduced by the coefficient of the effective shear area k_s and parameter r_{g1} by Kolmar (12) as follows: $G_{12}^{cr}=G_o.r_{g1}$, $G_{13}^{cr}=G_o.r_{g1}$, $G_{23}^{cr}=G_o/k_s$

When the tensile stress in the 2-direction reaches the value f_t', the latter cracked plane perpendicular to the first one is assumed to form, and the stress-strain relationship becomes:

$$\begin{Bmatrix} \sigma_1 \\ \sigma_2 \\ \tau_{12} \\ \tau_{13} \\ \tau_{23} \end{Bmatrix}_l = \begin{bmatrix} 0 & 0 & 0 & 0 & 0 \\ 0 & 0 & 0 & 0 & 0 \\ 0 & 0 & G_{12}^{cr}/2 & 0 & 0 \\ 0 & 0 & 0 & G_{13}^{cr} & 0 \\ 0 & 0 & 0 & 0 & G_{23}^{cr} \end{bmatrix}_l \begin{Bmatrix} \varepsilon_1 \\ \varepsilon_2 \\ \gamma_{12} \\ \gamma_{13} \\ \gamma_{23} \end{Bmatrix}_l \tag{11}$$

where the shear moduli are reduced by the parameter r_{g1} and r_{g2} by Kolmar (12) as follows:

$$G_{12}^{cr} = G_o.r_{g1}, \quad G_{13}^{cr} = G_o.r_{g1}, \quad G_{23}^{cr} = G_o r_{g2}.$$

The cracked concrete is anisotropic and these relations must be transformed to the reference axes XY. The simplified averaging process is more convenient for finite element formulation than the singular discrete model. A smeared representation for the cracked concrete implies that cracks are not discrete but distributed across the region of the finite element.

The smeared crack model (Oňate et al, 1988), used in this work, results from the assumption, that the field of more micro cracks (not one local failure) brought to the concrete element will be created. The validity of this assumption is determined by the size of the finite element, hence its characteristic dimension $L_c = \sqrt{A}$, where A is the element area (versus integrated point area of the element). For the expansion of cracking the assumption of constant failure energies G_f=*const* is proposed in the form

$$G_f = \int_0^\infty \sigma_n(w)dw = A_G.L_c, \qquad w_c = \varepsilon_w.L_c, \tag{12}$$

where w_c is the width of the failure, σ_n is the stress in the concrete in the normal direction, A_G is the area under the stress-strain diagram of concrete in tension. Concrete modulus for descend line of stress strain diagram in tension (crushing) can be described according to Oliver (Oňate et al, 1988) in dependency on the failure energies in the form

$$E_{c,s} = \frac{E_c}{1-\lambda_c}, \qquad \lambda_c = \frac{2G_f E_c}{L_c.\sigma_{\max}^2}, \tag{13}$$

where E_c is the initial concrete modulus elasticity, σ_{max} is the maximal stress in the concrete tension. From the condition of the real solution of the relation (13) it follows, that the characteristic dimension of element must satisfy the following condition

$$L_c \le \frac{2G_f E_c}{\sigma_{\max}^2}, \tag{14}$$

The characteristic dimension of the element is determined by the size of the failure energy of the element. The theory of a concrete failure was implied and applied to the 2D layered shell elements SHELL91 or SHELL281 in the ANSYS element library (Králik, 2002, 2009).

5. Nonlinear solution of the reinforced concrete BT wall

The reinforced concrete wall of the BT structure was modelled using the layered shell element with the smeared reinforcement and the steel liner (Králik, 2002, 2009). The limit of damage at a point was controlled by the values of the so-called crushing or total damage function F_u. The modified Kupfer's condition (Kupfer et al, 1969) for l - layer of section is following

$$F_u^l = F_u^l(I_{\varepsilon 1}; J_{\varepsilon 2}; \varepsilon_u) = 0, \qquad F_u^l = \sqrt{\beta\left(3J_{\varepsilon 2}\right) + \alpha I_{\varepsilon 1}} - \varepsilon_u = 0, \tag{15}$$

where $I_{\varepsilon 1}$, $J_{\varepsilon 2}$ are strain invariants, and ε_u is an ultimate total strain extrapolated from uniaxial test results, α, β are material parameters determined from Kupfer's experiment results ((β = 1,355, α = 0,355ε_u). In the rotated crack model (Králik, 2002, 2009), the direction of the principal stress coincides with the direction of the principal strain. If the principal strain axes rotate during the loading the direction of the cracks rotates, too. In order to ensure the coaxiality of the principal strain axes with the material axes the tangent shear modulus G_t is calculated as

$$G_t = \frac{\sigma_{c1} - \sigma_{c1}}{2\left(\varepsilon_1 - \varepsilon_2\right)} \tag{16}$$

The CRACK program was used for the nonlinear analysis of the BT reinforced concrete structure (Králik, 2002, 2009).

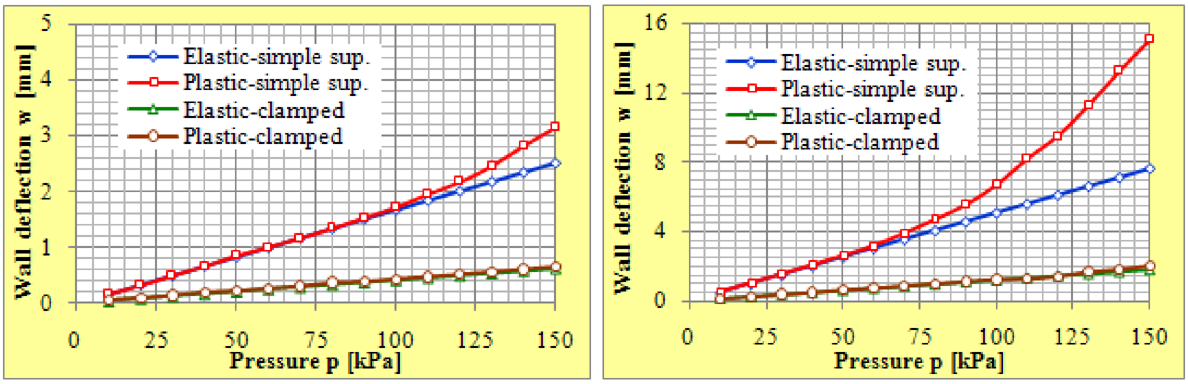

Figure 12 Comparison the displacement of the wall segment of BT gas-tank 1 and 4 for elastic and plastic solution

The comparison of the influences of the plastic deformation and boundary effects is presented in the Fig.12. Two walls were considered – the wall of the 1th and 4th gas-tank. The wall of the 1th gas-tank (i.e. 4th gas-tank) has dimension 39,0/10,65/1,5m (i.e. 39,0/13,61/1,5m). The simple support and clamped was investigated. Also, the elastic and plastic behavior of concrete material was considered too.

5. Conclusion

This paper presented the results from the experimental and numerical investigation of the safety and reliability of the BT structure (Králik, 2009). The experimental test was realized for the pressure 100kPa. The numerical solution was carrying out for the pressure 100kPa and 150kPa. The BT structure was checked for the BDBA load case in accordance of the IAEA requirements (IAEA, 1995).

Table 3 Deflection of the concrete plates of BT structures under pressure 150kPa

	Roof pate at level +50,6m			Concrete wall in modulus *E* (up)		
	Numerical Analysis		Experiment	Numerical Analysis		Experiment
Load case	w_{tot} [mm]	w_{rel} [mm]	Extrapolation	w_{tot} [mm]	w_{rel} [mm]	Extrapolation
Pressure 150kPa	6,175	5,279	4,461	2,446	0,387	1,645
BDBA combin.	4,196	4,751	-	8,788	1,848	-

The maximum values of the deflections from the numerical analysis and experiment were compared in table 3. It is necessary to tell that the temperature into interior is equal to 50°C and in exterior 25 °C in the case of the BDBA load (Králik, 2002, 2009).

4. Acknowledgement

The project was realized with the financial support of the Grant Agency of the Slovak Republic (VEGA). The project registration number is VEGA 1/0849/08.

5. References

Červenka V. (1985) Constitutive Model for Cracked Reinforced Concrete, *ACI Journal*, pp. 877-882.

Eurocode 1990 (2002) Basis of Structural Design. ENV 1991-1-1, CEN.

Eurocode 1992 (1990), Design of Concrete Structures, Part 1, CEC.

FISA99 (1999) "Containment evaluation under severe accidents (CESA) –synthesis of the predictive calculations and analysis of the first experimental results obtained on the Civuax mock-up", European Commission, Conclusion symposium on shared cost and concerted actions, Rep. EUR 19532, pp 510-519.

IAEA (1995) *Guidelines for WWER 440/213 Containment Evaluation*, Rep. IAEA, March.

Janotka, L. Nűrnbergerová, T. (1999) Concrete Behaviour in Mochovce Reactor Envelope at Temperatures up to 200°C, *Building Research Journal*, 47/2, str. 143-161.

Jerga, J. Križma, M. (2006) Assessment of Concrete Damage, *Building Research Journal*, 54(3-4), pp. 211-220.

Juriš, P. Jančovič, J. (2006) Accident Iniciated by Leak Coolant Medium for EMO1,2. LOCA 2X500MM. VÚJE,A.S. V01-TS/2871/0220/2006.15.

Kolmar, W. (1986) Beschreibung der Kraftuebertragung ueber Risse in nichtlinearen Finite-Element-Berechnungen von Stahlbetontragwerken, PhD Thesis, T.H. Darmstadt, pp 94.

Králik, J. Cesnak, J. (2001) Nonlinear Analysis of Power Plant Buildings with the VVER 230 Reactor after a Loss off Coolant Accident. In: *Slovac Journal of Civil Engineering*. Slovak University of Technology Bratislava, Vol. 3, pp.18-32.

Králik, J. (2002) Experimental and Numerical Analysis of Reinforced Concrete Containment after Loss of Coolant Accident, In proc. *The International Symposium on "Mechanics of Composites"*, October 14, Prague, Czech Republic, CTU in Prague, pp.91-98.

Králik, J. (2002a) Safety and Reliability Analysis of Concrete Containment Considering Concrete Cracking Due to Loss Coolant Accident, *Engineering Structures*, Alfa Bratislava, roč.50, č.3, pp. 19-25.

Králik, J. (2009) *Safety and Reliability of Nuclear Power Buildings in Slovakia. Earthquake – Impact - Explosion*. Ed. STU Bratislava, 2009, 307 pp.

Kupfer H., Hilsdorf H.K., Ruesch H. (1969) Behavior of Concrete Under Biaxial Stresses, *Journal ACI 66* (8), August, pp.656-666.

Materna, A. Salajka, V. Brdečko, L. (2000) Calculation Models for the Nonlinear Solution of Reinforced Structures. In: *Nonlinear mechanics, III. Slovak-Polish-Czech symposium of mechanics*, SvF STU Bratislava, October, pp.113-116.

NUREG-1150 (1990) *Severe Accident Risks: An Assessment for Five US Nuclear Power Plants*, Summary Report, Final Summary Report, NUREG-1150, Vol.1 and 2, December.

Oňate E., Oller S., Oliver J. and Lubliner J. (1988) A Constitutive Model for Cracking of Concrete Based on the Incremental Theory of Plasticity, Eng. Comput. 5(2).

Řeřicha, P. Šejnoha, J. (2008) Partial Service Life Assessment of a Reactor Containment, *Nuclear Engineering Design* 235, p.2451-2462.